



Single-walled carbon nanotubes: synthesis and quantitative purification evaluation by acid/base treatment for high carbon impurity elimination

Afsoon Aghaei¹ · Maryam Shaterian¹ · Hassan Hosseini-Monfared² · Afsaneh Farokhi¹

Received: 10 March 2022 / Accepted: 7 September 2022 / Published online: 17 September 2022
© Institute of Chemistry, Slovak Academy of Sciences 2022

Abstract

Purification of carbon nanotubes by chemical oxidation method and their efficiency was considered a function of the position and size of the catalyst residues and thus the morphology of the tubes. Reproducible, low loss and high-yield purification procedure for single-walled carbon nanotubes (SWCNTs) was expanded by acid–base treatment with nitric acid and sodium hydroxide. Herein, we have described high SWCNTs growth and selectivity due to optimal metal-support interaction in iron oxide nanoparticles/alumina ($\text{Fe}_2\text{O}_3/\text{Al}_2\text{O}_3$) catalyst by chemical vapor deposition technique under CH_4 gas. Then, SWCNTs obtained over metallic catalyst can be efficiently purified by liquid oxidation method. The process involves the NaOH treatment at temperatures of 100 °C for 6 h, which remove the support particles, and an acid treatment with HNO_3 for 1 h, which etches away the catalytic metals. The quality of the final material was verified by Fourier transform infrared, Raman spectroscopy, energy-dispersive X-ray (EDS), thermogravimetric analysis and transmission electron microscopy. The results showed that the amorphous carbon and iron catalysts were completely removed without any damage to the walls of structure. Our research shows that this method can greatly enhance the selectivity of carbonaceous impurities removal.

Keywords Single-walled carbon nanotube · $\text{Fe}_2\text{O}_3/\text{Al}_2\text{O}_3$ · Purification · Liquid oxidation · NaOH/ HNO_3

Introduction

Single-walled carbon nanotubes (SWCNTs) are one-dimensional structures and possess many unique mechanical, electrical, thermal and optical properties (Z. J. Han et al. 2012). This makes the SWCNTs networks among the most outstanding products for various applications including nanoelectronics and energy solar cells, storage devices, biosensors and several others (Z. Han and Ostrikov 2010). SWCNTs are generally synthesized by three common methods containing arc discharge (Journet et al. 1997), laser ablation (Guo et al. 1995) and chemical vapor deposition (CVD), which are the catalytic decomposition of hydrocarbon on transition metals at elevated temperatures (Andrews et al. 2006;

Ghosh et al. 2007; M. Kumar and Ando 2003; R. Kumar et al. 2011). The CVD process is one of the main techniques for industrial large scale (Fathy 2017). The SWCNTs nucleation and growth are impressed by many factors such as catalyst, pressure, gas, and temperature (Fisher et al. 2011). Different sources carbon in gas-form were used extensively as SWCNTs precursors such as methane (CH_4), carbon monoxide (CO), ethanol ($\text{CH}_3\text{CH}_2\text{OH}$), and ethylene (C_2H_4) (Liu et al. 2010). Various types of supports like magnesia (MgO), silica (SiO_2), alumina (Al_2O_3), zeolite, and mesoporous materials such as MCM-41 are used for SWCNTs production (Wenelska and Mijowska 2019). Catalytic synthesis is one of the most popular methods to control the selectivity SWCNTs with high yield and comparatively low cost (Lim et al. 2003). The widest catalysts applied for fabrication of SWCNTs are transition metals such as iron, cobalt, and nickel (Zhang et al. 2014). Previous reports have shown the SWCNTs diameters are quite similar to diameters of catalytic nanoparticles (Yiming Li et al. 2001). Sakurai et al. 2012 have shown that small nanoparticles (iron as a catalyst in an AlOx support layer) are suitable for SWCNTs growth and produce a high performance, long length, high surface

✉ Afsoon Aghaei
afsoon.aghayi@znu.ac.ir

¹ Department of Chemistry, Faculty of Science, University of Zanjan, 45195-313, Zanjan, Iran

² Department of Chemistry, Amirkabir University of Technology, Tehran, Iran

area, and alignment. The SWCNTs usually contain carbonaceous fragments such as transition metals, amorphous carbon, and graphitic nanoparticles, and thus these impurities avoid their applications. Many purification methods have been developed which can be classified into four main methods: acid oxidation (Ribeiro et al. 2021; Rinzler et al. 1998), gas oxidation (Goak et al. 2020b; Zimmerman et al. 2000), chromatography (Duesberg et al. 1998) and filtration (Yu Li et al. 2004). The most frequently utilized agent, the simplest and most useful method for oxidation of carbon nanotubes, is refluxing with nitric acid (Jeynes et al. 2008; Tchoul et al. 2007).

In this paper, we have described SWCNTs growth by iron oxide nanoparticles/alumina ($\text{Fe}_2\text{O}_3/\text{Al}_2\text{O}_3$) catalyst by CVD technique under CH_4 gas. The iron compound acts as a specific catalyst for the growth of SWCNTs, when alumina is as a support. The current synthesis method does not allow any pre-treatment of the catalyst precursor to make an active catalyst precursor by using H_2 gas. Hence, our work avoids toxic chemicals and harmful gases such as H_2 , CO , etc. Additionally, it is an ecologically beneficial and oxidant material that may be an impressive precursor for SWCNTs development. This research attempts to find a less destructive chemical for the purification of SWCNTs. Thus, the research would examine the effect of nitric acid and sodium hydroxide for purification. This method preferentially purifies without introducing sidewall defects and shortening of the chain length.

Experimental

Synthesis of iron-oleate (Fe-oleate) complex

A Fe-oleate complex was prepared including sodium oleate and iron chlorides. Sodium oleate was obtained by reacting sodium hydroxide anhydrous and oleic acid. At first 0.088 g sodium hydroxide anhydrous (2.2 mmol) and 0.62 g oleic acid (2.2 mmol) were dissolved in 7 ml distilled water and stirred for 2 h at 65 °C. Then 0.2 g of iron chloride (0.74 mmol) and 0.67 g of sodium oleate (2.2 mmol) were added to a mixture of distilled water (6 ml), ethanol (8 ml), and hexane (14 ml). The brown-orange solution is refluxed for 4 h at 70 °C. After completion of the reaction, the upper organic phase including the Fe-oleate complex was washed four times with 4 ml deionized water in a separatory funnel. Finally, Hexane was vaporized after washing and Fe-oleate was formed in the solid form of wax (Park et al. 2004).

Synthesis of Fe_2O_3 nanoparticles

For the synthesis of Fe_2O_3 particles, 0.34 g of Fe-oleate (0.5 mmol) and 0.24 g of glycerol (2 mmol) were blended

in 10 ml of ethanol at room temperature. The combination was annealed to 180 °C at a steady heating rate of 10 °C/min and then held at this temperature for 30 min. As the reaction continued, the primary brown clear solution became black-brown. After the reaction, the compound was quickly cooled to room temperature, and the precipitate of the nanoparticles was formed by the addition of 5 mL acetone. Fe_2O_3 were isolated by centrifugation and dispersed in non-polar solvents such as n-hexane or chloroform (Kim et al. 2011).

Synthesis of $\text{Fe}_2\text{O}_3/\text{Al}_2\text{O}_3$

The detailed manner for preparing the catalyst is as follows: 2 ml of dispersed Fe_2O_3 solution in chloroform and 2 ml DMF were stirred at room temperature for 3 days. Then 1.2 g Al_2O_3 (11 mmol) was added to the solution at room temperature for 3 h. The temperature of the solution was kept at 50 °C until a lot of precipitation was produced. The precipitation was dried for 3 h at 150 °C. The catalyst with weight ratio ($\text{Fe}_2\text{O}_3/\text{Al}_2\text{O}_3 = 1:16$) was obtained.

Growth of SWCNTs

The SWCNTs were grown at 1000 °C using $\text{Fe}_2\text{O}_3/\text{Al}_2\text{O}_3$ as a catalyst by CVD method (Fig. 1). $\text{Fe}_2\text{O}_3/\text{Al}_2\text{O}_3$ (761 mg) was placed in a boat located in the middle of the quartz reactor. The temperature of the CVD reactor increased to 1000 °C under the N_2 gas flow at 60 sccm during a period of 100 min. At 1000 °C, CH_4 gas was passed through the reactor at 160 sccm for 30 min to grow the nanotubes. After growth, the CVD system was cooled to room temperature in a N_2 environment. It is worth mentioning that mass flow controllers (MFCs) were used to control the flow of gases (Billing et al. 2018).

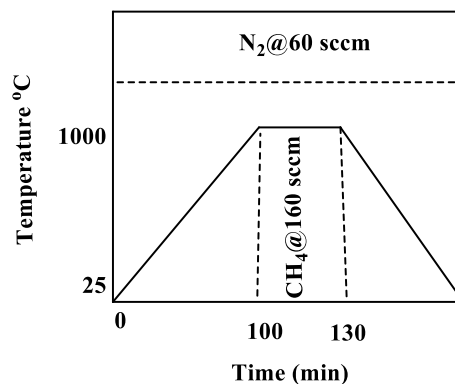


Fig. 1 Growth protocol used to production SWCNTs in a CVD reactor

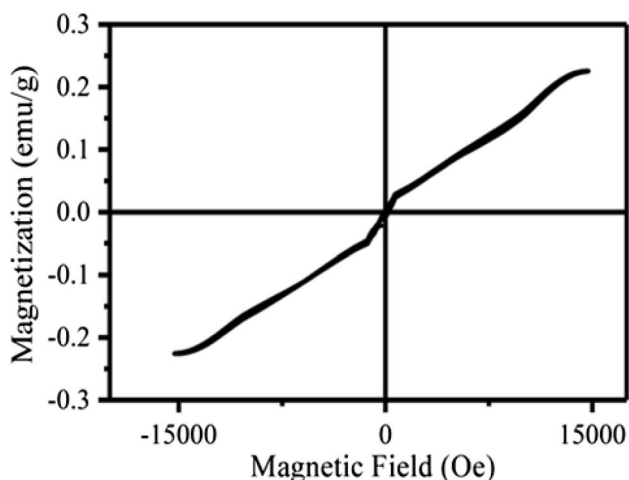
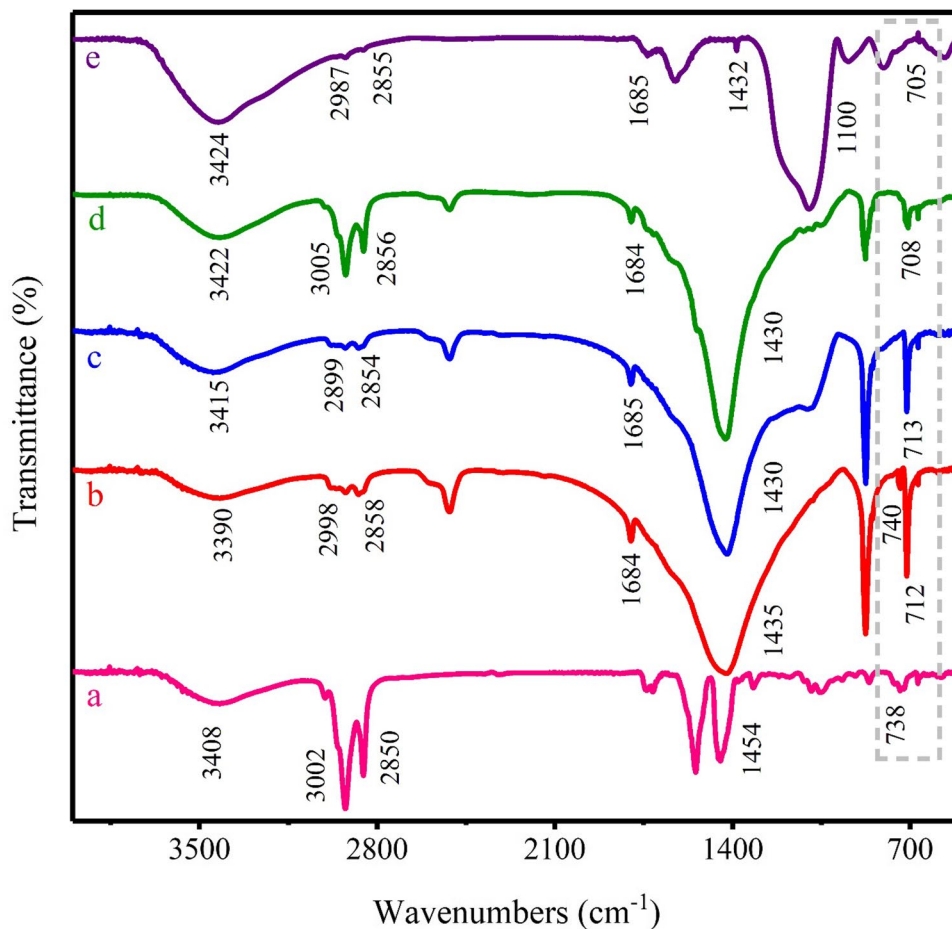


Fig. 2 Hysteresis loops for the Fe_2O_3

Purification of SWCNTs

The raw product was purified with refluxing in 6 M NaOH for 6 h and 6 M HNO_3 solutions for 1 h at 100 °C to eliminate the support and Fe_2O_3 particles, respectively. After NaOH treatment sample washing with deionized water.

Fig. 3 FT-IR analysis of a Fe_2O_3 b SWCNTs c base treatment d acid treatment e acid/base treatment



Lastly, the purified SWCNTs were washed with distilled water and dried for 12 h at 110 °C (Boskovic et al. 2013).

Characterization techniques

The morphology and structure of Fe_2O_3 was studied using scanning electron microscopy (SEM) analysis (Hitachi, s4160, Japan). Transmission electron microscopy (TEM) images were carried out on a (Philips, cm30, Netherlands). X-ray powder diffraction (XRD) analysis was recorded on PANalytical X'PERTPRO diffractometer using $\text{Cu K}\alpha$ radiation ($\lambda = 1.54$ angstrom, 40 kV, 30 mA). Fourier transform infrared (FT-IR) spectroscopic measurements (Mattson 1000 spectrophotometer) were reported from 400 to 4000 cm^{-1} . The sample palette was built in KBr and the background spectra were subtracted from the sample spectra to ensure that the actual sample was analyzed. The Raman spectrum of the SWCNTs has been collected by the Takram P50C0R10 Raman spectrometer with an excitation wavelength of 532 nm. The magnetic characterization was recorded by a vibrating sample magnetometer (VSM: magnetic daghigh kavir, model MDKB) with a maximum magnetic field about 2 Tesla at room temperature. The

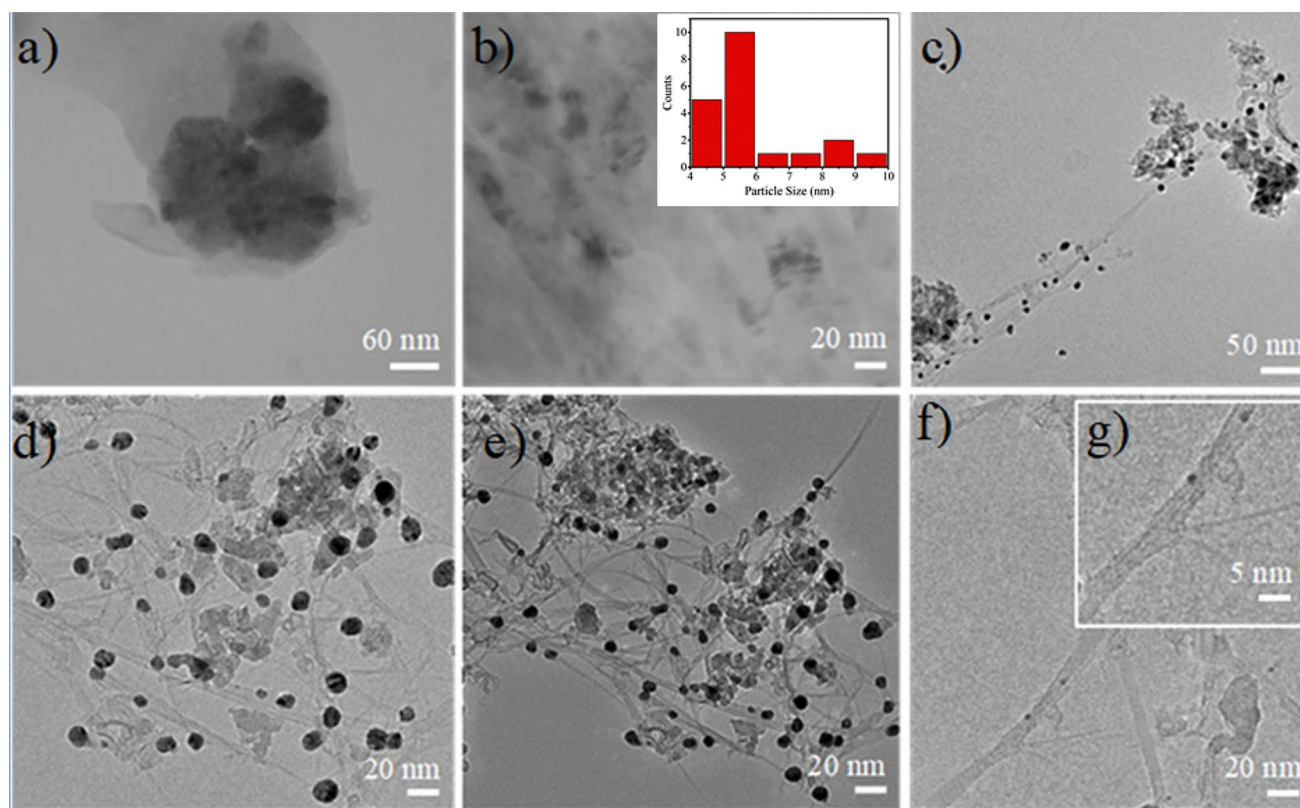


Fig. 4 a, b TEM image of Fe_2O_3 in different scales and the inset displays particle size distribution c–e raw SWCNTs sample f, g purified SWCNTs

elemental structure was analyzed using energy-dispersive X-ray spectroscopy (EDS) analysis (MIRAIII, TESCAN, Czechia). Thermal stability has been studied by thermogravimetric analysis (TGA) (STA 504 model, German company BHR) under air and argon atmosphere from zero temperature to 1000 °C.

Results and discussion

VSM analysis

Magnetization measurements of Fe_2O_3 nanoparticles were performed by using a VSM with the magnetic field up to 2T (Fig. 2). Magnetic properties are mostly related to the particle size (Goya et al. 2003). As a result, small magnetic nanoparticles contain very small magnetic moments and have shown an approximately linear relationship between magnetization and magnetic field, that is very close to the magnetic property of paramagnetic materials (Jiles 2015; Lee and Hyeon 2012).

FT-IR analysis

The FT-IR spectra of Fe_2O_3 nanoparticles, SWCNTs and purified SWCNTs are shown in Fig. 3. Absorption bands located at 3002, 2921, and 2850 cm^{-1} in the spectrum of the Fe_2O_3 nanoparticles are ascribed to the stretching vibrations of $\nu(\text{CH})$ olefinic, $\nu_{\text{asymmetric}}(\text{CH}_2)$ and $\nu_{\text{symmetric}}(\text{CH}_2)$ of oleic acid, whereas the bands at 738 cm^{-1} correspond to the Fe–O stretching vibration (Adireddy et al. 2009; Bayazit et al. 2015; Kwon et al. 2007; Park et al. 2004). These groups were used in the preparation of Fe-oleate and consequently the production of Fe_2O_3 particles. The adsorption bands located at 1435 cm^{-1} and 1684 cm^{-1} are characteristic bands of aromatic C=C. Bands at 1300–1000 cm^{-1} are related to C–O stretching which indicate the surface of SWCNTs has some oxygen including functional groups because NaOH/ HNO_3 . The band 738 cm^{-1} in the spectrum of purified SWCNTs, that is removed compared with SWCNTs, is related to the Fe–O bond after NaOH treatment (Fig. 3c) (Kysil et al. 2017; Levin and Brandon 1998). Figure 3d shows SWCNTs treated with HNO_3 solution to remove Al_2O_3 . This process

Table 1 Comparison of the conditions used for the purification of SWCNTs

Entry	Sample	Material	Reaction temp (°C)/time (h)	Drying temp. (°C)/time (h)	Purity wt%	Carbon yield	Characterization	References
1	SWCNTs	3 M HNO ₃ 7 M HNO ₃	refluxed/12 Refluxed/6	R.T R.T	69 65	–	Vis–NIR, TGA, SEM	Hu et al. (2003)
2	Commercial SWCNT	Oxidized + 4 M HNO ₃	Sonication/2	303 k/overnight	94	–	TGA	Shobin and Manivannan (2018)
3	CNT	3 M NaOH 3 M HNO ₃	Refluxed/6 Refluxed/6	110/24 h	–	240	TEM, EDS, BET	Boskovic et al. (2013)
4	SWCNTs	3 M HNO ₃ + oxidized	120/6	70/overnight	21.1	–	SEM, TEM Raman TGA UV–Vis–NIR	Goak et al. (2020a)
5	CNT	3 M NaOH 3 M HNO ₃	Refluxed/6 Refluxed/6	110/24 h	–	264/62	TEM, TG, DTG, XRD, DSC, Raman	Ratkovic et al. (2014)
6	SWCNTs	1.5 M HNO ₃	210/30 min	105/48	98.40	–	TGA DTG Raman	Yuca and Karatepe (2011)
7	SWCNTs	Concentrated HNO ₃	Refluxed/24	100/30 min	–	~95%	XRD, SEM, TEM, HRTEM, TGA, IR, Raman	Leela Mohana Reddy and Ramaprabhu (2007)
8	SWCNT	2.6 M HNO ₃	125/48	60/48	–	94.2%	ATR-IR, XPS, TGA, Raman	Bergeret et al. (2008)
9	SWCNTs	14 M HNO ₃	100/4	Overnight	35	–	TEM TG, DTG, DTA Absorption	Ma and Wang (2008)
10	SWCNTs	3 M HNO ₃ /oxidized	Refluxed/16	Overnight	–	66.2	TEM, Raman	Shen et al. (2005)
11	SWCNTs	6 M HNO ₃	Refluxed/12	100/overnight	89.3	–	Raman, TEM TGA, SEM	Clancy et al. (2016)
12	SWCNTs	6 M HNO ₃	120/8	105/48	98.29	10 to 20	TGA,	Belyakov (2019)
13	CNTs	6 M HNO ₃	80/36	Overnight	7.00	10.82	TEM, EDS, TGA	Pumera (2007)
14	SWCNTs	concentrated HNO ₃	Refluxed/1.5	–	108	–	Near-IR, Raman, Mid-IR, TGA, TEM	Worsley et al. (2009)
15	DWCNTs	3 M HNO ₃	130/24	80/overnight	82	–	TEM, FTIR, AFM	Bortolamiol et al. (2014)
16	SWCNTs	6 M NaOH 6 M HNO ₃	100/6 100/1	110/12	–	7.1	TEM, FTIR, Raman, EDS, TGA	Present work

effectively removed support. But in general, the simultaneous effect of NaOH/HNO₃ is needed for significant and efficient removal, as seen from the results of Fig. 3e. As a result, a large amount of impurities and catalyst support were successfully separated by the acid/base digestion purification method.

SEM and TEM analysis

The average crystalline size and morphology of the Fe₂O₃ nanoparticles, SWCNTs and purified SWCNTs were determined by TEM images. Figure 4a, b displays the Fe₂O₃

particles with mainly spherical form and an average particle size of 5–6 nm (Shukoor et al. 2007). Figure 4c, d shows images of growth and purified SWCNTs by refluxing in NaOH (6 M) for 6 h at 100 °C and in HNO₃ (6 M) for 1 h at 100 °C. In addition to the bundle of nanotubes, the dark and gray spots structure in Fig. 4d comes from the support and metallic nanoparticles. Figure 4f, g shows unremarkable changes from the raw sample, indicating that acid/base treatment is sufficient. The decrease in the amount of impurities, as indicated by gray and black groups, is unobserved on the surface of the bundle of nanotubes. These results showed that by choosing the appropriate method and time, impurities

can be selectively removed from nanotubes. Therefore, the key to producing high-quality purified SWCNTs with high performance is acid/base reflux (Mattevi et al. 2008; Noda et al. 2007). SEM analysis shows the morphology of Fe_2O_3 . This micrograph indicated (see Fig. S1 in ESI†) highly uniform grains distribution.

The main problem in the purification of SWCNTs by acid/base treatment is the loss of a large number of nanotubes due to inappropriate conditions. Table 1 compares the purification conditions of SWCNTs in NaOH/ HNO_3 solutions. The present research includes advantages such as: high efficiency, easy operation, short time, no damage to SWCNTs, and low consumption of reagents. But in other methods, the purification efficiency decreased with increasing temperature, acid concentration and time. Among all the methods of SWCNTs reported in Table 1, our work has the highest efficiency with 6 M NaOH/ HNO_3 for 6/1 h at 100 °C.

XRD analysis

XRD analysis was used to display the crystal structure of the nanoparticle. XRD pattern of Fe_2O_3 has shown mostly maghemite ($\gamma\text{-Fe}_2\text{O}_3$) crystal structure (Fig. S2 in ESI†). Although it is difficult to distinguish between magnetite and maghemite, the XRD pattern is similar to that of maghemite due to their very similar XRD patterns. All the diffraction peaks of nano-particles are consistent with the standard structure (JCPDS card No. 39-1346). The results indicated that the products consisted of pure phases (Table S1 in ESI†) (Hyeon et al. 2001; Kim et al. 2011; Rahman et al. 2014).

Raman spectroscopy and energy-dispersive X-ray

Raman spectroscopy (Fig. 5) and energy-dispersive X-ray (Fig. 6) identified the growth and purity of SWCNTs. Figure 5a, b displays the *G*-band, *D*-band and radial breathing mode (RBM) of raw and purified SWCNTs. The RBMs are composed of lower frequencies in the range between 200 and 400 cm^{-1} , which frequencies depend on the tube diameters. Moreover, RBM is an important part giving further structural information for (*n*, *m*) assignments, such as on the chirality in SWCNTs. The RBM bands can be detected at 248.85, 273.90 and 286.40 cm^{-1} . Therefore, it is possible to devote the bands to the (12,0), (9,3) and (9,2) chirality under the excitation energy of 2.33 eV (532 nm), respectively (Hiura et al. 1993; Moon et al. 2001). Raw and pure SWCNTs show a band at around 1589 and 1590 cm^{-1} assigned to *G* band. The *G* band detached into two components (Dresselhaus et al. 2010). These two distinct bands include (G^+), which are caused by the vibration of carbon atoms along the nanotube axis, and (G^-), which are motivated by the vibration of carbon atoms along the peripheral direction of SWCNTs. These bands was observed in the regions of 1590, 1588,

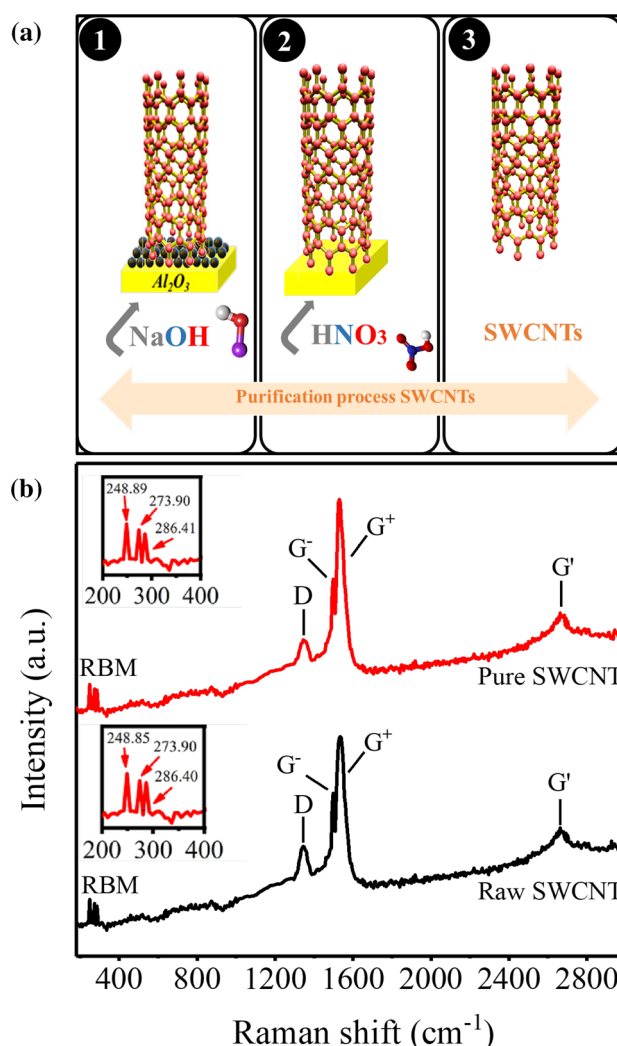


Fig. 5 a Protocol for the purification of SWCNTs b Raman spectra of raw and purified SWCNTs at 532 nm laser excitations

1558 and 1557 cm^{-1} , respectively (Saito et al. 2011). An additional band is considered near 1345 and 1344 cm^{-1} called *D* band, which is related with defects or disorder in SWCNTs, such as amorphous carbon and heteroatoms. The origin of the *D* band is thought to be a double-resonance process. The *G'* band, which is the overtone of the *D* band, is located at around 2667 and 2661 cm^{-1} . The ratio of the *D* and *G*-bands intensities distinguish relative defect content in the carbon lattice. The decrease in the intensity ratio of *D* and *G*-band (*ID*/*IG*) after purification indicates the quality of SWCNTs (Hou et al. 2017; Otsuka et al. 2014; Wunderlich et al. 2008).

TGA

TGA analysis is a beneficial technique to evaluate the structure, purity and thermal stability of SWCNTs along with

Fig. 6 **a** EDX analysis of raw SWCNTs **b** EDX analysis for purified SWCNTs

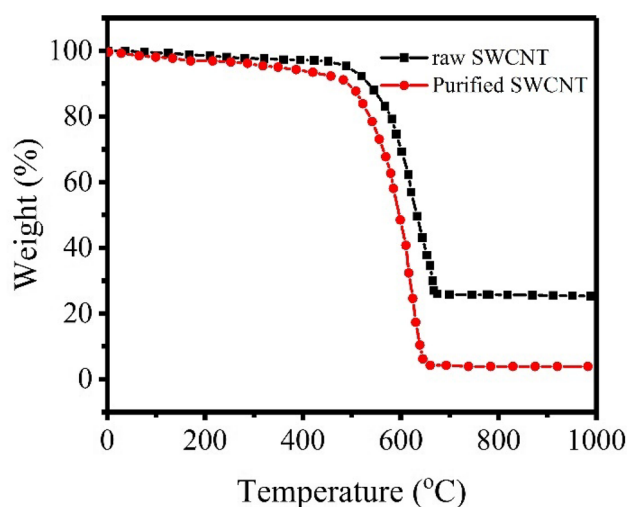
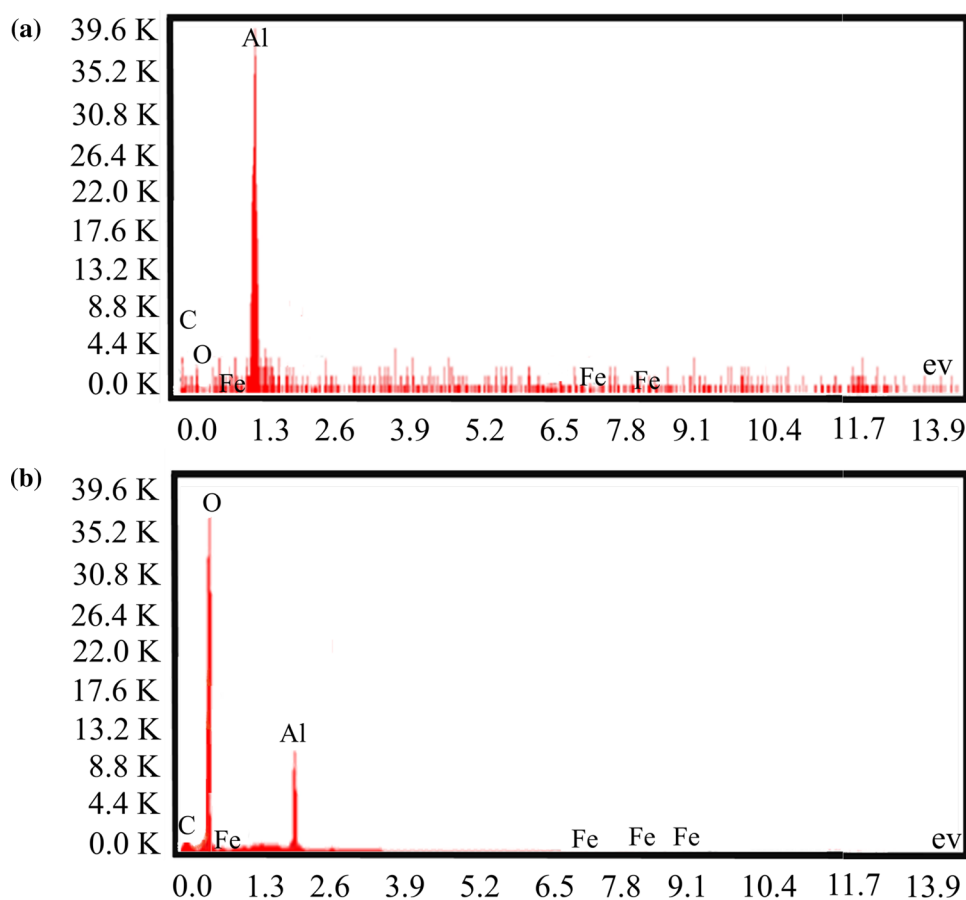


Fig. 7 TGA of raw and purified SWCNTs

the content of residual impurities. Figure 7 shows the TGA study of the raw and purified SWCNTs. The remaining impurities in raw SWCNTs are ~25%. There is no considerable weight loss before 400 °C, so there is a significant amount of impurities. In the purified SWCNTs, the greatest

rate of impurities removes up at 650 °C. As a result, after acid/base treatment the impurity amount is decreased to less than 5% (Matsuzawa et al. 2014).

Conclusions

Purification of SWCNTs materials depends on the removal of impurities such as metal and carbon impurities, so that the structure of the actual SWCNTs remains intact. A uniform nanoparticle was formed by controlled thermal decomposition of the Fe-oleate complex. The SWCNTs is grown using $\text{Fe}_2\text{O}_3/\text{Al}_2\text{O}_3$ as a catalyst without the presence of hydrogen gas under CH_4 gas. The SWCNTs are notable for having a narrow diameter distribution and chirality (12,0), (9,3) and (9,2). This nanotube can be efficiently purified by NaOH/HNO_3 treatment. The TEM images display purified SWCNT free of carbon impurities and metals. The great quality of SWCNTs was defined by the (ID/IG) as shown in Raman spectroscopy. In this method, the purification time is shortened and modified effectively. As a result, nanotubes with a small diameter are not destroyed. The general availability of purified SWCNTs makes it possible to understand their potentially

attractive applications as well as to understand their fundamental properties.

Supplementary Information The online version contains supplementary material available at <https://doi.org/10.1007/s11696-022-02478-5>.

Acknowledgements The authors thank the University of the Zanjan for research funds.

Data availability The data that support the findings of this study are available in the supplementary material of this article.

Declarations

Conflict of interest The authors declare that they have no conflict of interest.

References

- Adireddy S, Lin C, Palshin V, Dong Y, Cole R, Caruntu G (2009) Size-controlled synthesis of quasi-monodisperse transition-metal ferrite nanocrystals in fatty alcohol solutions. *Phys Chem C* 113(49):20800–20811. <https://doi.org/10.1021/jp905955k>
- Andrews RJ, Smith CF, Alexander AJ (2006) Mechanism of carbon nanotube growth from camphor and camphor analogs by chemical vapor deposition. *Carbon* 44(2):341–347. <https://doi.org/10.1016/j.carbon.2005.07.025>
- Bayazit M, Pålsson L, Coleman K (2015) Sensing properties of light-emitting single walled carbon nanotubes prepared via click chemistry of ylides bound to the nanotube surface. *RSC Adv* 5(46):36865–36873. <https://doi.org/10.1039/C5RA04330A>
- Belyakov A (2019) Carbon nanotubes for the synthesis of ceramic matrix composites (cleaning, dispersion, surface modification). *Refract Ind Ceram* 60(1):92–100. <https://doi.org/10.1007/s11148-019-00315-z>
- Bergeret C, Cousseau J, Fernandez V, Mevellec J-Y, Lefrant S (2008) Spectroscopic evidence of carbon nanotubes' metallic character loss induced by covalent functionalization via nitric acid purification. *J Phys Chem C* 112(42):16411–16416. <https://doi.org/10.1021/jp806602t>
- Billing BK, Dhar P, Singh N, Agnihotri PK (2018) Augmenting static and dynamic mechanical strength of carbon nanotube/epoxy soft nanocomposites via modulation of purification and functionalization routes. *Soft Matter* 14(2):291–300. <https://doi.org/10.1039/C7SM01768E>
- Bortolamiol T, Lukanov P, Galibert A-M, Soula B, Lonchambon P, Datas L, Flahaut E (2014) Double-walled carbon nanotubes: quantitative purification assessment, balance between purification and degradation and solution filling as an evidence of opening. *Carbon* 78:79–90. <https://doi.org/10.1016/j.carbon.2014.06.051>
- Boskovic G, Ratkovic S, Kiss E, Geszti O (2013) Carbon nanotubes purification constrains due to large Fe–Ni/Al 2 O 3 catalyst particles encapsulation. *Bull Mater Sci* 36(1):1–7. <https://doi.org/10.1007/s12034-013-0435-6>
- Clancy AJ, White ER, Tay HH, Yau HC, Shaffer MS (2016) Systematic comparison of conventional and reductive single-walled carbon nanotube purifications. *Carbon* 108:423–432. <https://doi.org/10.1016/j.carbon.2016.07.034>
- Dresselhaus MS, Jorio A, Saito R (2010) Characterizing graphene, graphite, and carbon nanotubes by Raman spectroscopy. *Annu Rev Condens Matter Phys* 1(1):89–108. <https://doi.org/10.1146/annurev-conmatphys-070909-103919>
- Duesberg G, Burghard M, Muster J, Philipp G (1998) Separation of carbon nanotubes by size exclusion chromatography. *Commun Chem* 3:435–436. <https://doi.org/10.1039/A707465D>
- Fathy NA (2017) Carbon nanotubes synthesis using carbonization of pretreated rice straw through chemical vapor deposition of camphor. *RSC Adv* 7(45):28535–28541. <https://doi.org/10.1039/C7RA04882C>
- Fisher C, Han Z, Levchenko I, Ostrikov K (2011) Control of dense carbon nanotube arrays via hierarchical multilayer catalyst. *Appl Phys Lett* 99(14):143104. <https://doi.org/10.1063/1.3645625>
- Ghosh P, Afre RA, Soga T, Jimbo T (2007) A simple method of producing single-walled carbon nanotubes from a natural precursor: eucalyptus oil. *Mater Lett* 61(17):3768–3770. <https://doi.org/10.1016/j.matlet.2006.12.030>
- Goak JC, Lee SH, Lee N (2020a) Effect of purification on the electrical properties of transparent conductive films fabricated from single-walled carbon nanotubes. *Diam Relat Mater* 106:107815
- Goak JC, Lee SH, Lee N (2020b) Effect of purification on the electrical properties of transparent conductive films fabricated from single-walled carbon nanotubes. *Diam Relat Mater* 106:107815. <https://doi.org/10.1016/j.diamond.2020.107815>
- Goya GF, Berquo T, Fonseca F, Morales M (2003) Static and dynamic magnetic properties of spherical magnetite nanoparticles. *J Appl Phys* 94(5):3520–3528. <https://doi.org/10.1063/1.1599959>
- Guo T, Nikolaev P, Thess A, Colbert DT, Smalley RE (1995) Catalytic growth of single-walled nanotubes by laser vaporization. *Chem Phys Lett* 243(1–2):49–54. [https://doi.org/10.1016/0009-2614\(95\)00825-O](https://doi.org/10.1016/0009-2614(95)00825-O)
- Han Z, Ostrikov K (2010) Controlled electronic transport in single-walled carbon nanotube networks: selecting electron hopping and chemical doping mechanisms. *Appl Phys Lett* 96(23):233115. <https://doi.org/10.1063/1.3449118>
- Han ZJ, Mehdipour H, Li X, Shen J, Randeniya L, Yang HY, Ostrikov K (2012) SWCNT networks on nanoporous silica catalyst support: morphological and connectivity control for nanoelectronic, gas-sensing, and biosensing devices. *ACS Nano* 6(7):5809–5819. <https://doi.org/10.1021/nn302020a>
- Hiura H, Ebbesen T, Tanigaki K, Takahashi H (1993) Raman studies of carbon nanotubes. *Chem Phys Lett* 202(6):509–512. [https://doi.org/10.1016/0009-2614\(93\)90040-8](https://doi.org/10.1016/0009-2614(93)90040-8)
- Hou B, Wu C, Inoue T, Chiashi S, Xiang R, Maruyama S (2017) Extended alcohol catalytic chemical vapor deposition for efficient growth of single-walled carbon nanotubes thinner than (6, 5). *Carbon* 119:502–510. <https://doi.org/10.1016/j.carbon.2017.04.045>
- Hu H, Zhao B, Itkis ME, Haddon RC (2003) Nitric acid purification of single-walled carbon nanotubes. *J Phys Chem B* 107(50):13838–13842. <https://doi.org/10.1021/jp035719i>
- Hyeon T, Lee SS, Park J, Chung Y, Na HB (2001) Synthesis of highly crystalline and monodisperse maghemite nanocrystallites without a size-selection process. *J Am Chem Soc* 123(51):12798–12801. <https://doi.org/10.1021/ja016812s>
- Jeynes J, Jeynes C, Kirkby K, Rummeli M, Silva S (2008) RBS/EBS/PIXE measurement of single-walled carbon nanotube modification by nitric acid purification treatment. *Nucl Instrum Methods Phys Res B Beam Interact Mater Atoms* 266(8):1569–1573. <https://doi.org/10.1016/j.nimb.2007.12.105>
- Jiles D (2015) Introduction to magnetism and magnetic materials. CRC Press
- Journet C, Maser W, Bernier P, Loiseau A, de La Chapelle ML, Lefrant DS, Fischer J (1997) Large-scale production of single-walled carbon nanotubes by the electric-arc technique. *Nature* 388(6644):756–758. <https://doi.org/10.1038/41972>

- Kim BH, Lee N, Kim H, An K, Park YI, Choi Y, Na HB (2011) Large-scale synthesis of uniform and extremely small-sized iron oxide nanoparticles for high-resolution T1 magnetic resonance imaging contrast agents. *J Am Chem Soc* 133(32):12624–12631. <https://doi.org/10.1021/ja203340u>
- Kumar M, Ando Y (2003) Camphor—a botanical precursor producing garden of carbon nanotubes. *Diam Relat Mater* 12(3–7):998–1002. [https://doi.org/10.1016/S0925-9635\(02\)00341-2](https://doi.org/10.1016/S0925-9635(02)00341-2)
- Kumar R, Tiwari RS, Srivastava ON (2011) Scalable synthesis of aligned carbon nanotubes bundles using green natural precursor: neem oil. *Nanoscale Res Lett* 6(1):1–6. <https://doi.org/10.1186/1556-276X-6-92>
- Kwon SG, Piao Y, Park J, Angappane S, Jo Y, Hwang N-M, Hyeon T (2007) Kinetics of monodisperse iron oxide nanocrystal formation by “heating-up” process. *J Am Chem Soc* 129(41):12571–12584. <https://doi.org/10.1021/ja074633q>
- Kysil D, Vasin A, Sevostianov S, Degoda VY, Strelchuk V, Naseka V, Lysenko V (2017) Formation and luminescent properties of Al₂O₃: SiOC nanocomposites on the base of alumina nanoparticles modified by phenyltrimethoxysilane. *Nanoscale Res Lett* 12(1):1–5. <https://doi.org/10.1186/s11671-017-2245-z>
- Lee N, Hyeon T (2012) Designed synthesis of uniformly sized iron oxide nanoparticles for efficient magnetic resonance imaging contrast agents. *Chem Soc Rev* 41(7):2575–2589. <https://doi.org/10.1039/C1CS15248C>
- Leela Mohana Reddy A, Ramaprabhu S (2007) Pt/SWNT–Pt/C nanocomposite electrocatalysts for proton-exchange membrane fuel cells. *J Phys Chem C* 111(44):16138–16146. <https://doi.org/10.1021/jp066985+>
- Levin I, Brandon D (1998) Metastable alumina polymorphs: crystal structures and transition sequences. *J Am Ceram Soc* 81(8):1995–2012. <https://doi.org/10.1111/j.1151-2916.1998.tb02581.x>
- Li Y, Kim W, Zhang Y, Rolandi M, Wang D, Dai H (2001) Growth of single-walled carbon nanotubes from discrete catalytic nanoparticles of various sizes. *J Phys Chem B* 105(46):11424–11431. <https://doi.org/10.1021/jp012085b>
- Li Y, Zhang X, Luo J, Huang W, Cheng J, Luo Z, Ke X (2004) Purification of CVD synthesized single-wall carbon nanotubes by different acid oxidation treatments. *Nanotechnology* 15(11):1645. <https://doi.org/10.1088/0957-4484/15/11/047>
- Lim S, Ciuparu D, Pak C, Dobek F, Chen Y, Harding D, Haller G (2003) Synthesis and characterization of highly ordered Co-MCM-41 for production of aligned single walled carbon nanotubes (SWNT). *J Phys Chem B* 107(40):11048–11056. <https://doi.org/10.1021/jp0304778>
- Liu S, Shen Q, Cao Y, Gan L, Wang Z, Steigerwald ML, Guo X (2010) Chemical functionalization of single-walled carbon nanotube field-effect transistors as switches and sensors. *Coord Chem Rev* 254(9–10):1101–1116. <https://doi.org/10.1016/j.ccr.2009.11.007>
- Ma J, Wang JN (2008) Purification of single-walled carbon nanotubes by a highly efficient and nondestructive approach. *Chem Mater* 20(9):2895–2902. <https://doi.org/10.1021/cm8001699>
- Matsuzawa Y, Takada Y, Kodaira T, Kihara H, Kataura H, Yoshida M (2014) Effective nondestructive purification of single-walled carbon nanotubes based on high-speed centrifugation with a photochemically removable dispersant. *J Phys Chem C* 118(9):5013–5019. <https://doi.org/10.1021/jp411964z>
- Mattevi C, Wirth CT, Hofmann S, Blume R, Cantoro M, Ducati C, Castellarin-Cudia C (2008) In-situ X-ray photoelectron spectroscopy study of catalyst– support interactions and growth of carbon nanotube forests. *J Phys Chem C* 112(32):12207–12213. <https://doi.org/10.1021/jp802474g>
- Moon J-M, An KH, Lee YH, Park YS, Bae DJ, Park G-S (2001) High-yield purification process of singlewalled carbon nanotubes. *J Phys Chem B* 105(24):5677–5681. <https://doi.org/10.1021/jp0102365>
- Noda S, Hasegawa K, Sugime H, Kakehi K, Zhang Z, Maruyama S, Yamaguchi Y (2007) Millimeter-thick single-walled carbon nanotube forests: hidden role of catalyst support. *Jpn J Appl Phys* 46(5L):L399. <https://doi.org/10.1143/JJAP.46.L399>
- Otsuka K, Inoue T, Chiashi S, Maruyama S (2014) Selective removal of metallic single-walled carbon nanotubes in full length by organic film-assisted electrical breakdown. *Nanoscale* 6(15):8831–8835. <https://doi.org/10.1039/C4NR01690D>
- Park J, An K, Hwang Y, Park J-G, Noh H-J, Kim J-Y, Hyeon T (2004) Ultra-large-scale syntheses of monodisperse nanocrystals. *Nat Mater* 3(12):891–895. <https://doi.org/10.1038/nmat1251>
- Pumera M (2007) Carbon nanotubes contain residual metal catalyst nanoparticles even after washing with nitric acid at elevated temperature because these metal nanoparticles are sheathed by several graphene sheets. *Langmuir* 23(11):6453–6458. <https://doi.org/10.1021/la070088v>
- Rahman MU, Usman M, Hasanain SK, Ullah A, Kim IW (2014) Static magnetic properties of maghemite nanoparticles. *J Korean Phys Soc* 65(11):1925–1929. <https://doi.org/10.3938/jkps.65.1925>
- Ratkovic S, Peica N, Thomsen C, Bukur DB, Boskovic G (2014) Thermal stability evolution of carbon nanotubes caused by liquid oxidation. *J Therm Anal Calorim* 115(2):1477–1486. <https://doi.org/10.1007/s10973-013-3441-4>
- Ribeiro H, Schnitzler MC, da Silva WM, Santos AP (2021) Purification of carbon nanotubes produced by the electric arc-discharge method. *Surf Interfaces* 26:101389. <https://doi.org/10.1016/j.surfin.2021.101389>
- Rinzler AG, Liu J, Dai H, Nikolaev P, Huffman CB, Rodríguez-Macías FJ, Smalley RE (1998) Large-scale purification of single-wall carbon nanotubes: process, product, and characterization. *Appl Phys A* 67(1):29–37. <https://doi.org/10.1007/s003390050734>
- Saito R, Hofmann M, Dresselhaus G, Jorio A, Dresselhaus M (2011) Raman spectroscopy of graphene and carbon nanotubes. *Adv Phys* 60(3):413–550. <https://doi.org/10.1080/00018732.2011.582251>
- Sakurai S, Nishino H, Futaba DN, Yasuda S, Yamada T, Maigne A, Hata K (2012) Role of subsurface diffusion and Ostwald ripening in catalyst formation for single-walled carbon nanotube forest growth. *J Am Chem Soc* 134(4):2148–2153. <https://doi.org/10.1021/ja208706c>
- Shen K, Curran S, Xu H, Rogelj S, Jiang Y, Dewald J, Pietrass T (2005) Single-walled carbon nanotube purification, pelletization, and surfactant-assisted dispersion: a combined TEM and resonant micro-Raman spectroscopy study. *J Phys Chem B* 109(10):4455–4463. <https://doi.org/10.1021/jp045046j>
- Shobin LR, Manivannan S (2018) Enhancement of electrothermal performance in single-walled carbon nanotube transparent heaters by room temperature post treatment. *Sol Energy Mater Sol Cells* 174:469–477. <https://doi.org/10.1016/j.solmat.2017.09.041>
- Shukoor MI, Natalio F, Ksenofontov V, Tahir MN, Eberhardt M, Theato P, Tremel W (2007) Double-stranded RNA polyinosinic-polycytidylic acid immobilized onto γ -Fe₂O₃ nanoparticles by using a multifunctional polymeric linker. *Small* 3(8):1374–1378. <https://doi.org/10.1002/sml.200600664>
- Tchoul MN, Ford WT, Lolli G, Resasco DE, Arepalli S (2007) Effect of mild nitric acid oxidation on dispersability, size, and structure of single-walled carbon nanotubes. *Chem Mater* 19(23):5765–5772. <https://doi.org/10.1021/cm0717581>
- Wenelska K, Mijowska E (2019) Exfoliated molybdenum disulfide as a platform for carbon nanotube growth-properties and characterization. *ACS Omega* 4(6):10225–10230. <https://doi.org/10.1021/acsomega.8b03425>
- Worsley KA, Kalinina I, Bekyarova E, Haddon RC (2009) Functionalization and dissolution of nitric acid treated single-walled carbon nanotubes. *J Am Chem Soc* 131(50):18153–18158. <https://doi.org/10.1021/ja906267g>

- Wunderlich D, Hauke F, Hirsch A (2008) Preferred functionalization of metallic and small-diameter single walled carbon nanotubes via reductive alkylation. *J Mater Chem a* 18(13):1493–1497. <https://doi.org/10.1039/B716732F>
- Yuca N, Karatepe N (2011) Hydrogen storage in single-walled carbon nanotubes purified by microwave digestion method. *World Acad Eng Technol* 79:605–610. <https://doi.org/10.5281/zenodo.1055120>
- Zhang L, Hou P-X, Li S, Shi C, Cong H-T, Liu C, Cheng H-M (2014) In situ TEM observations on the sulfur-assisted catalytic growth of single-wall carbon nanotubes. *J Phys Chem Lett* 5(8):1427–1432. <https://doi.org/10.1021/jz500419r>
- Zimmerman JL, Bradley RK, Huffman CB, Hauge RH, Margrave JL (2000) Gas-phase purification of single-wall carbon nanotubes.

J Mater Chem 12(5):1361–1366. <https://doi.org/10.1021/cm990693m>

Publisher's Note Springer Nature remains neutral with regard to jurisdictional claims in published maps and institutional affiliations.

Springer Nature or its licensor holds exclusive rights to this article under a publishing agreement with the author(s) or other rightsholder(s); author self-archiving of the accepted manuscript version of this article is solely governed by the terms of such publishing agreement and applicable law.